

Field and Accelerated Aging of Cracked Solar Cells

Michael G. Deceglie ¹, Member, IEEE, Timothy J Silverman ², Senior Member, IEEE, Ethan Young, William B. Hobbs ³, Senior Member, IEEE, and Cara Libby ⁴, Member, IEEE

Abstract—Cracks can form in silicon solar cells in an otherwise intact photovoltaic module due to mechanical stresses such as rough handling or hail. The immediate impact on power due to these cracks can be readily measured, but it is also known from accelerated testing that the cracks can worsen over time. However, it is not clear how to predict the extent of future field degradation due to cracked cells, which requires a calibrated accelerated test. We describe progress toward such a test. In particular, we report on the outdoor aging of modules with cracked cells for nearly two years. We find that modules with cracked cells degraded in the field an average of 0.5% absolute more than uncracked modules over a period of 21 months. We also characterize the modules with multitemperature electroluminescence and find that the degradation is associated with cell fragments that become electrically isolated. We compare the weathering outdoors with the two types of accelerated tests: thermal cycling and a novel accelerated test, dynamic mechanical acceleration (DMX). DMX can apply thousands of pressure cycles at a frequency of approximately 10 Hz and pressures <200 Pa, which are relevant to the wind-driven pressure cycles experienced by modules outdoors. We find that the thermal cycles designed to reproduce the cumulative temperature change from the field overestimate field degradation and can excite noncell-crack degradation. DMX results were promising, reproducing degradation levels similar to those observed outdoors over 21 months with a test that can be performed in less than an hour.

Index Terms—Accelerated testing, electroluminescence (EL), photovoltaic cells, reliability, solar panels.

I. INTRODUCTION

SILICON (Si) solar cells break within otherwise intact photovoltaic (PV) modules for a variety of reasons, including handling, transportation, and weather, such as hail. Mechanical

Manuscript received 6 June 2023; revised 28 July 2023; accepted 21 August 2023. Date of publication 19 September 2023; date of current version 7 November 2023. This work was supported in part by National Renewable Energy Laboratory, operated by Alliance for Sustainable Energy, LLC, for the U.S. Department of Energy (DOE), under Grant DE-AC36-08GO28308, in part by Durable Modules Consortium (DuraMAT), an Energy Materials Network Consortium funded by the U.S. Department of Energy, Office of Energy Efficiency and Renewable Energy, Solar Energy Technologies Office, under Grant 32509, and in part by the U.S. Department of Energy Office of Energy Efficiency and Renewable Energy Solar Energy Technologies Office under Grant 38263. (Corresponding author: Michael G. Deceglie.)

Michael G. Deceglie, Timothy J Silverman, and Ethan Young are with the National Renewable Energy Laboratory, Golden, CO 80401 USA (e-mail: michael.deceglie@nrel.gov; timothy.silverman@nrel.gov; ethan.young@nrel.gov).

William B. Hobbs is with the Southern Company, Birmingham, AL 35203 USA (e-mail: whobbs@southernco.com).

Cara Libby is with the Electric Power Research Institute, Palo Alto, CA 94304 USA (e-mail: cllibby@epri.com).

Color versions of one or more figures in this article are available at <https://doi.org/10.1109/JPHOTOV.2023.3309933>.

Digital Object Identifier 10.1109/JPHOTOV.2023.3309933

flaws introduced during manufacturing can predispose cells to crack under these stresses. Power loss due to cell cracks is a two-stage process. In the first stage, the crack in the Si is formed. In the second stage, electrical contact with cell fragments is reduced or lost as the metallization grid lines across the crack fail or degrade. In some cases, these two stages may happen in immediate succession, but in others, the second stage may take time to occur as environmental stressors cause cell fragments to shift.

It is well established that electrical isolation of cracked cell fragments can increase in extreme weather and with the application of accelerated tests, including thermal cycles or mechanical load [1], [2], [3]. Field degradation associated with cracks has also been observed [4]. However, it is unclear how the weathering of cracked cells manifests under typical moderate conditions in the field. Many studies of cracked modules in the field involve modules that have been cracked for an unknown amount of time, making the quantification of the weathering (the second stage in power loss) challenging. Furthermore, this weathering is likely product dependent, creating the need for an accelerated test to quantify the future aging of modules once they become cracked.

We describe results that build toward such a field-relevant accelerated test for the weathering of cracked cells. In the experiment, we precracked modules and deployed them outdoors for nearly two years along-side uncracked control modules. In parallel, we subjected both intact and precracked modules of the same types deployed outdoors to the novel dynamic mechanical acceleration (DMX) test [5] and accelerated thermal cycling.

DMX is based on the observation that pressure cycles experienced by PV modules due to wind (hundreds of Pa) are generally well below the pressures of existing standardized mechanical load tests (thousands of Pa), while also much higher in cycle count [6], [7]. The technique uses an array of speakers to apply field-relevant pressure cycles at ~ 10 Hz, allowing the accumulation of years of field damage in hours of testing. Approximately 10 Hz was chosen to be below the resonance of the DMX-module system to avoid destruction of the DMX apparatus and irrelevantly large laminate displacements. To the best of authors' knowledge, other apparatuses for applying dynamic mechanical loading, which rely on an array of suction cups controlled by actuators or a means (other than speakers) of controlling the pressure in a cavity around the module [8], cannot achieve frequencies as high as 10 Hz.

The thermal cycling test was designed to test the hypothesis that reproducing the same total change in temperature (ΔT) observed outside, including small fluctuations, would reproduce the relevant cell fragment movement and, thus, cracked-cell weathering.

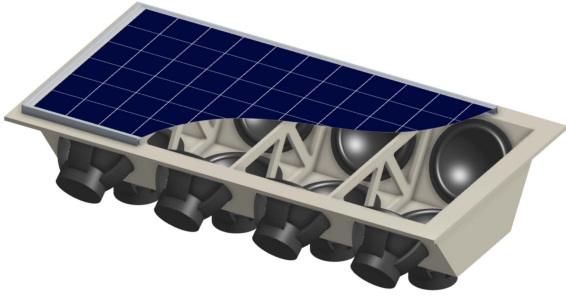


Fig. 1. DMX apparatus, which uses an array of speakers to apply field-relevant pressure cycles (<500 Pa) at 10 Hz. (Si module pictured as schematic cut away to show DMX internal components.) © IEEE 2022 [5].

II. METHODS

The experiment focused on 72-cell multicrystalline Si modules of four different models from various manufacturers. In total, 16 modules (four of each type) were deployed outdoors on a single-axis tracker for 21 months in Golden, CO, USA. The tracker was on the western edge of a ten-tracker field. To the west, there was a south-facing fixed-tilt PV array. The hub height of the tracker was approximately 1.4 m. Modules were individually maximum power tracked with dc optimizers. Cells within the modules were intentionally cracked on eight of the 16 modules (two of each type) prior to deployment. The cracks were induced in the cells by dropping one edge of the module from a height that cracked approximately 1/3 of the cells in a simulated “installer drop.” This height varied by module type, and was determined from sacrificial trial modules not used for further study, but with the module constructions being quite similar, we did not observe a systematic difference between drop height and module design. The glass remained intact.

In parallel legs of the experiment, six modules from three of the types deployed outdoors underwent accelerated testing with the DMX method [5] and with thermal cycling. Testing was limited to three types due to the limited sample count of the fourth type. Similarly to the outdoor leg of the experiment, cells in half of the modules in the accelerated testing legs were intentionally cracked with a simulated “installer drop.”

One of the accelerated testing legs investigated DMX, which uses an array of speakers driven at approximately 10 Hz to apply mechanical pressure cycles similar to those experienced outdoors in typical wind conditions. The method is described in more detail in [5], and a diagram of the DMX apparatus is shown in Fig. 1. In the version of DMX used in this study, the entire module frame is constrained to the apparatus, which is expected to cause different stress profiles than field mounting; newer versions of the apparatus are being developed, which enable field-relevant mounting. We exposed the modules to two successive levels of DMX derived from 2-D computational fluid dynamics simulations of wind levels measured at the test site [9]. We picked the DMX levels based on pressure (rather than module displacement) in order to naturally capture differences in the module response between different module types. We also acknowledge that in the field, the frequency content of the excitation will be different than that of DMX, but the storage modulus

of different encapsulants changes only marginally over the range 0.1–100 Hz [10] minimizing this concern. The storage modulus does, however, change appreciably with temperature [10], making the choice to perform DMX only at room temperature a larger simplifying assumption. Even so, we hypothesized that the simplification to a 10 Hz excitation at room temperature would be sufficiently representative to induce field-relevant degradation, and test this hypothesis with the experiments described herein. Using 20 years of historical wind speed data at 1-min resolution measured at the site [11], the two DMX levels were designed to correspond to the windiest noncontiguous day and windiest noncontiguous hour experienced at the site in a year at the wind measurement height of 6.7 m, these speeds were 14 and 21 m/s. Relative to the windiest day, fewer cycles but higher pressure are needed to reproduce the windiest hour. The cycle count for each level was doubled to represent the approximately two years of outdoor exposure in this experiment. The first level (DMX 1) was 346 000 cycles of 70 Pa rms pressure cycles and the second level (DMX 2) was 22 000 cycles of 150 Pa rms cycles.

The other accelerated testing leg focused on thermal cycling using an environmental chamber. We designed the thermal cycles to reproduce the same total change in temperature, ΔT , experienced by the modules outdoors, including small fluctuations that occur throughout the day. We calculated the total ΔT from 1-min thermocouple measurements collected on the rear side of fielded modules for one calendar year according to

$$\Delta T = \sum_i T(t_i) - T(t_{i-1}) \quad (1)$$

where $T(t_i)$ is the discrete temperature measurement at time (t_i). Because the surface module temperature fluctuates faster than the cell temperature inside the module, we applied an exponentially weighted moving average (EWMA) with a constant (α) of 0.56 before calculating the total temperature change from the discrete differences of the EWMA time series. The EWMA constant was found by comparing a back-of-module temperature with a cell temperature on a custom mini module deployed outdoors for one week with a thermocouple on the cell surface inside the laminate. We optimized the EWMA constant such that the ΔT calculated from the EWMA of the exterior of the module matched that of the interior.

Using this approach, we found a total ΔT for each year of exposure was 8.35×10^4 °C. We also observed that the median daily range of temperatures experienced by the module spanned 40 °C. Finally, we found that the 10th percentile of daytime temperature was approximately 10 °C and the 90th percentile was approximately 50 °C. The exact choice of these percentile is somewhat arbitrary, but ensures that the accelerated thermal cycles occur in the temperature regime relevant to outdoor operation. Combining these observations, we targeted 1044 full cycles from 10 °C to 50 °C for each year of exposure. Our chamber could achieve approximately 13 cycles per day. Due to limitations in the equipment and lack of a dwell at the extremes of the cycles, the minimum module temperature of the modules in the chamber fluctuated between 10 °C and 15 °C during cycling. We added additional cycles at the end of each test to achieve a total observed ΔT of 8.35×10^4 °C (the ΔT for 1044 cycles

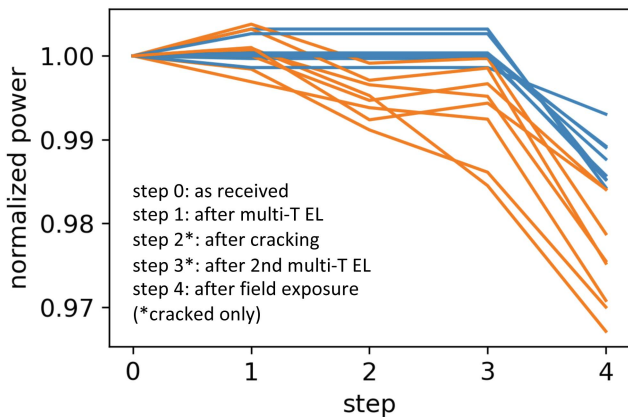


Fig. 2. Power loss on cracked (orange) and uncracked (blue) modules fielded outdoors after each step of the experiment. Cracked modules degraded more quickly outdoors than uncracked modules.

from 10 °C to 50 °C). We carried out two consecutive rounds of thermal cycling in this way; we refer to them as TC 1 and TC 2. To summarize, each round of thermal cycling (TC 1 and 2) was designed to reproduce the outdoor ΔT of a single year of deployment in Golden, CO USA.

Between experimental steps, modules were characterized by multitemperature electroluminescence (EL) and room temperature current–voltage (I – V) curves. Room temperature I – V curves were collected at 25 °C using a Spire 5600 flash simulator.

We use multitemperature EL to fully characterize the state of a module with cracked cells over the full range of relevant temperatures. As cell fragments of a broken cell move with thermal expansion and contraction, the lateral resistance across the crack changes [12]. We image the module in an environmental chamber at 10 °C increments from –15 °C to 65 °C and back down to –15 °C. At each incremental temperature, we collect an EL image at the rated I_{sc} using identical exposure settings. The gray values in each image are then normalized to their 90th percentile to account for changes in EL brightness with temperature. Finally, a composite image is formed by aligning all the normalized images and selecting the minimum value for each pixel. This composite image represents the worst-case scenario for each pixel and enables us to identify areas that become electrically disconnected over the range of outdoor-relevant temperatures.

III. RESULTS AND DISCUSSION

The results show that modules with cracked cells degraded more quickly outdoors than those without cracked cells. Fig. 2 shows the change in normalized power for modules in the outdoor leg of the experiment as measured by laboratory-based I – V curves for both cracked and uncracked modules after each step in the experiment. The spread in the data at step 1 is attributed to the uncertainty in the measurement and potentially changes in small cracks not detected in EL, since a single thermal cycle on intact modules is not expected to have a measurable effect. For the cracked modules, we observed an initial reduction in power <1% immediately after the cracks were introduced (experimental

step 2). The spread in the power for these modules then increases with the single round of multitemperature EL. This is likely due to cell fragments moving during the single thermal cycle associated with multitemperature EL. After outdoor deployment, the total degradation in the cracked modules was greater than that in the uncracked. We note that outdoor degradation for all the modules includes likely light-induced degradation, so it is possible that the degradation rate would slow in subsequent years. The median outdoor power loss calculated from the difference in the power measurements between experimental steps 4 and 3 (or step 1, for uncracked modules) was approximately 0.5% absolute more for the cracked population than for the uncracked population after 21 months of outdoor exposure.

Fig. 3 shows the results of multitemperature EL of the cracked modules before and after outdoor exposure. We observe an increase in the dark areas after outdoor weathering indicating more cell areas that are partially or fully isolated from the module circuit due to cell cracks. The range of outdoor power loss experienced by the modules relative to the average power loss observed in the uncracked control modules of the same make and model was –0.27% to 1.27% (positive values indicate degradation).

Fig. 4 shows the multitemperature EL along with the degradation in maximum power at one sun observed after each level of DMX testing. We observe cumulative degradation of 0.24% to 0.74% after both levels of DMX. Most of this loss accumulates in the second level of DMX testing, which had higher pressure but fewer cycles than the first level. Similarly, Fig. 5 shows the multitemperature EL along with the maximum power degradation after the first round of thermal cycle testing. After the second round of thermal cycle testing, the total degradation ranged from 0.72% to 1.5%. For both types of accelerated testing, we generally observe an increase in the dark areas in EL indicating that cell fragments are becoming at least partially isolated from the module circuit.

The degradation observed in both types of accelerated testing is compared with the outdoor leg of the experiment in Fig. 6. The results shown in the figure indicate that DMX 2 (preceded by DMX 1) was most representative of outdoor degradation. DMX 1 substantially underestimated the outdoor degradation, while both levels of thermal cycling overestimated it.

It is perhaps surprising that reproducing the same total ΔT that the modules experienced outdoors caused more damage in the laboratory test, even for TC 1, which was designed to reproduce only one year. There are some important differences between the temperature changes outdoors and those in the accelerated test, which may explain the difference. First, the distribution of temperatures at which the ΔT is accumulated outdoors and in the accelerated test are different, and cell fragment movement is not linear in temperature [13]. Another important difference is that a large fraction of ΔT accumulated outdoors occurs in small cycles, while relatively large, uniform cycles are used indoors. This may lead to differences in the details of cell fragment movement, which is known to be hysteretic [12].

Modules experience both thermal cycling and mechanical cycling outdoors, so neither type of accelerated test fully reproduces the stress that occurs outdoors. Our accelerated tests

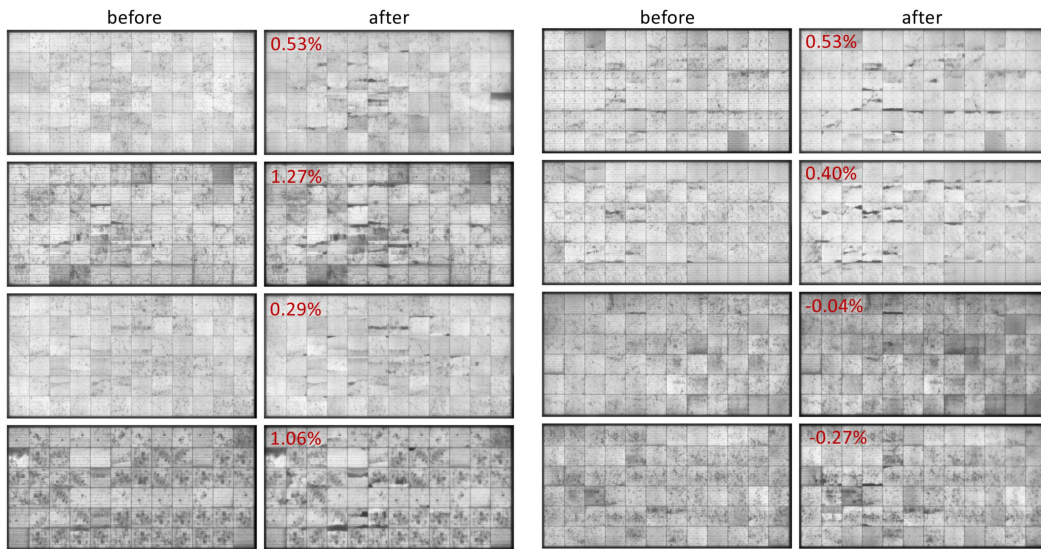


Fig. 3. Composite multitemperature EL images of the cracked modules from the outdoor leg of the experiment before and after deployment. The before images are taken after cracking but before outdoor exposure. The red numbers indicate the power loss each module experienced during the outdoor exposure relative to the average power loss in the uncracked control modules of the same make and model.

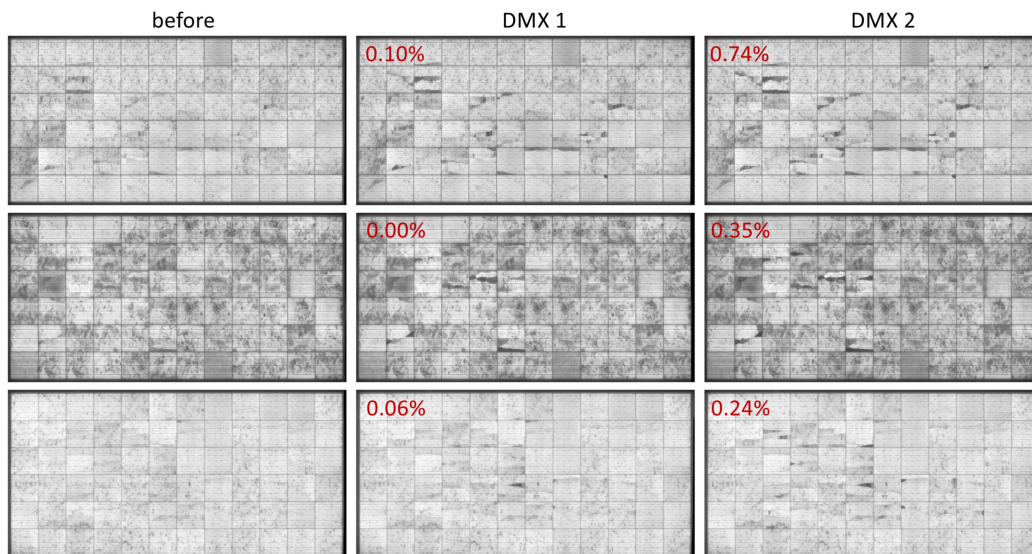


Fig. 4. Composite multitemperature EL images of cracked modules before and after each level of DMX testing. The before images are taken after cracking but before DMX. Each row corresponds to one module. The red numbers indicate the power loss observed from the corresponding DMX test.

show that both types of stress cause cracked cell damage to progress. In both cases, the single stressor applied by the test is implicitly used as a surrogate for the other. For example, DMX 2 (preceded by DMX 1) did enough damage to account for both the mechanical and thermal cycling that occurred outdoors, but using exclusively mechanical cycling. Although the results for DMX are promising, the exchange rate between the two stressors is not yet quantified. The temperature-dependent mechanical properties of different encapsulants in combination with the temperature realized in service conditions should be given careful consideration when quantifying these exchange rates [10], [14]. This must be better characterized before the

true acceleration factor of either type of test can be established. Quantifying the exchange rate between the two types of stress remains an important area of ongoing research.

We also observe that in the case of one module type, thermal cycling excited a degradation mode other than cell crack weathering. For the module type with five bus bars, the uncracked module experienced 0.69% power loss after TC 1 and a total of 0.98% after TC 2. This is similar to the degradation experienced by the cracked module of that type (bottom row of Figs. 4 and 5) which exhibited 0.88 and 1.11% degradation, respectively, in the two levels of thermal cycling. We also note that the temperature-dependent EL of the cracked module showed

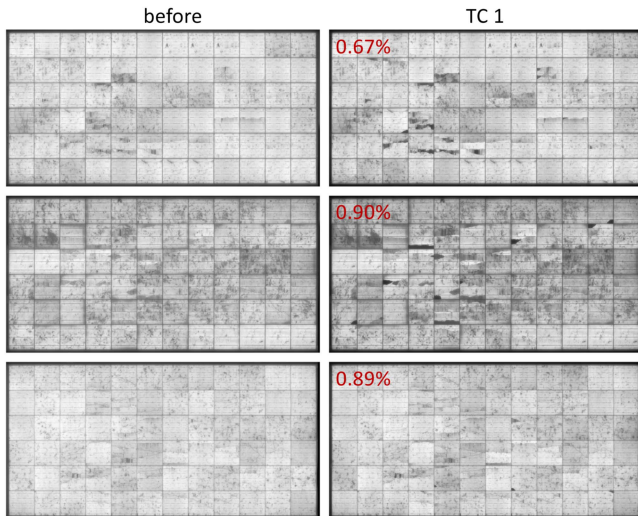


Fig. 5. Composite multitemperature EL images of cracked modules before and after the first level of thermal cycle testing. The before images are taken after cracking but before thermal cycling. Each row corresponds to one module. The red numbers indicate the power loss observed from the corresponding thermal cycle test.

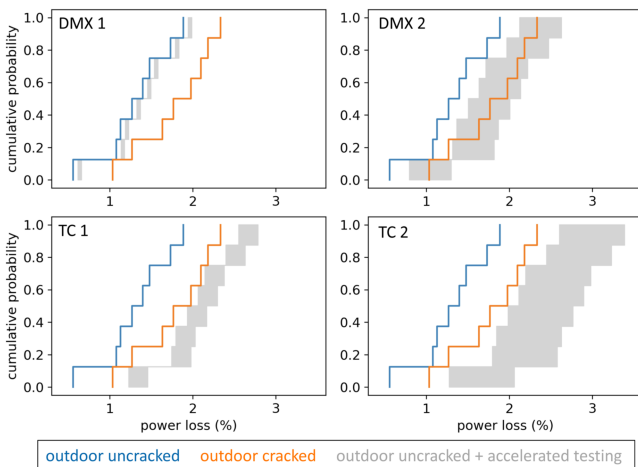


Fig. 6. Outdoor power loss compared with accelerated testing. Each panel shows the cumulative distribution function of the outdoor power loss for the uncracked set of modules (blue) and the cracked set (right). The gray area on each plot is calculated by adding the range of degradation values observed in the indicated accelerated test to the CDF of the outdoor uncracked set. This facilitates a comparison between the additional degradation of modules outdoors attributed to cracked cells and the degradation induced by accelerated testing. We observe that the DMX 2 (preceded by DMX 1) best represents the field degradation observed in this experiment.

only a minimal increase in dark areas after TC 1, as shown in Fig. 5, suggesting a different degradation mechanism is present. No obvious change was observed in the uncracked module's EL after thermal cycling. For reference, this module type appears in the first column rows 1 and 3 of Fig. 3.

IV. CONCLUSION

Cracked cells in otherwise intact modules are a well-known occurrence. The long-term performance risk posed by cracked cells has not previously been well understood. In this work,

we introduced cracks in a controlled way and used extensive characterization before and after field aging to show that cracked cells can, in fact, cause increased degradation in the field compared with the uncracked modules. We compared the outdoor aging with two types of accelerated testing, DMX and thermal cycling. We found that DMX 2 was promising in that it reproduced degradation levels similar to those observed in the field. However, we acknowledge that thermal cycling also occurs in the field and contributes to the field degradation. So some of the stress and degradation induced by DMX through mechanical cycles would be caused by thermal cycling outdoors. The exchange rate between the two types of stress is still poorly understood and remains an important area of continued research.

Although the exchange rate with thermal cycles is still poorly understood, we consider DMX to be a promising approach to accelerate cracked cell weathering. One reason is the time needed for the test. Each level of thermal cycling took approximately 80 days to complete, whereas DMX 2 took less than an hour to reproduce nearly two years of field weathering. Another reason that we consider DMX more promising than thermal cycles for this application is its specificity. In the case of one module type, thermal cycling apparently excited a degradation mode other than cracked-cell weathering. While DMX is promising, further work is needed to establish accurate acceleration factors to account for the thermal and mechanical cycles experienced in different field conditions.

It is not clear from the experimental results whether the crack weathering has saturated during outdoor exposure or if the degradation would continue at the same rate. However, the risk that it continues at the same rate is substantial; extrapolated to 20 years the crack degradation would cause an *additional* 11% degradation above and beyond the other degradation modes. Some anecdotal evidence suggests this risk is real. First, we have previously reported that after additional DMX cycles, well beyond what was applied in this study, crack damage continues [5]. Second, we observe areas of cells, which have the geometry to be electrically isolated, but remain in at least partial contact with the module circuit in the EL images of the outdoor-deployed modules of this study, indicating that there is potential for further increases in isolated areas in the future.

The modules studied here, multicrystalline Si with 3–5 busbars, are an older technology than what is being deployed today. However, our results are relevant to large numbers of multicrystalline systems still in service. The future underperformance risk of these systems is not yet well understood, and this study, including the application of DMX, provides a path to quantifying that future risk. Modern module designs with many busbars may mitigate the risks of long-term degradation by limiting the cell area that becomes isolated by cracks. Ultimately, crack weathering risk is product specific, and DMX is a promising approach to quickly quantify it.

ACKNOWLEDGMENT

The authors would like to thank Daniel Fregosi, Martin Springer, Michael Owen-Bellini, and Nick Bosco for insightful

discussions. The authors would also like to thank Allan Anderberg, Josh Gallon, Greg Perrin, Byron McDanold, Joshua Parker, Bill Sekulic, and Kent Terwilliger for help with experiments. The views expressed in the article do not necessarily represent the views of the DOE or the U.S. Government. The U.S. Government retains and the publisher, by accepting the article for publication, acknowledges that the U.S. Government retains a nonexclusive, paid-up, irrevocable, worldwide license to publish or reproduce the published form of this work, or allow others to do so, for U.S. Government purposes.

REFERENCES

- [1] M. Köntges, I. Kunze, S. Kajari-Schröder, X. Breitenmoser, and B. Bjørneklett, "The risk of power loss in crystalline silicon based photovoltaic modules due to micro-cracks," *Sol. Energy Mater. Sol. Cells*, vol. 95, no. 4, pp. 1131–1137, Apr. 2011.
- [2] H. Seigneur, E. Schneller, J. Lincoln, and A. M. Gabor, "Cyclic mechanical loading of solar panels—a field experiment," in *Proc. IEEE 7th World Conf. Photovolt. Energy Convers.*, 2018, pp. 3810–3814.
- [3] D. C. Jordan, K. Perry, R. White, and C. Deline, "Extreme weather and PV performance," *IEEE J. Photovolt.*, to be published, Aug. 21, 2023, doi: [10.1109/JPHOTOV.2023.3304357](https://doi.org/10.1109/JPHOTOV.2023.3304357).
- [4] R. Dubey et al., "Comprehensive study of performance degradation of field-mounted photovoltaic modules in India," *Energy Sci. Eng.*, vol. 5, no. 1, pp. 51–64, 2017. [Online]. Available: <https://onlinelibrary.wiley.com/doi/abs/10.1002/ese3.150>
- [5] T. J. Silverman, N. Bosco, M. Owen-Bellini, C. Libby, and M. G. Deceglie, "Millions of small pressure cycles drive damage in cracked solar cells," *IEEE J. Photovolt.*, vol. 12, no. 4, pp. 1090–1093, Jul. 2022.
- [6] C. Buerhop et al., "Evolution of cell cracks in PV-modules under field and laboratory conditions," *Prog. Photovolt.: Res. Appl.*, vol. 26, no. 4, pp. 261–272, 2018. [Online]. Available: <https://onlinelibrary.wiley.com/doi/pdf/10.1002/pip.2975>
- [7] M. Assmus, S. Jack, K.-A. Weiss, and M. Koehl, "Measurement and simulation of vibrations of PV-modules induced by dynamic mechanical loads: Measurement and simulation of vibrations of PV-modules," *Prog. Photovolt.: Res. Appl.*, vol. 19, no. 6, pp. 688–694, Sep. 2011.
- [8] E. J. Schneller et al., "Evaluating solar cell fracture as a function of module mechanical loading conditions," in *Proc. IEEE 44th Photovolt. Specialist Conf.*, 2017, pp. 2897–2901.
- [9] E. Young, M. Deceglie, and T. Silverman, "Computational methods to characterize panel loading conditions for accelerated testing," in *Proc. Photovolt. Rel. Workshop*, 2021. [Online]. Available: https://www.youtube.com/watch?v=h_yjCdK8aG0&t=5427s
- [10] N. Bosco, M. Springer, and X. He, "Viscoelastic material characterization and modeling of photovoltaic module packaging materials for direct finite-element method input," *IEEE J. Photovolt.*, vol. 10, no. 5, pp. 1424–1440, Sep. 2020.
- [11] T. Stoffel and A. Andreas, "NREL solar radiation research laboratory (SRRL): Baseline measurement system (BMS); Golden, Colorado (data)." [Online]. Available: <https://www.osti.gov/biblio/1052221>
- [12] T. J. Silverman, M. G. Deceglie, M. Owen-Bellini, W. B. Hobbs, and C. Libby, "Cracked solar cell performance depends on module temperature," in *Proc. IEEE 48th Photovolt. Specialists Conf.*, 2021, pp. 1691–1692.
- [13] M. Springer, T. J. Silverman, N. Bosco, J. Joe, and I. Repins, "Residual stresses affect cell fragment movement," *IEEE J. Photovolt.*, vol. 13, no. 4, pp. 547–551, Jul. 2023.
- [14] G. Mülhölfer, H. Berg, C. Ferrara, W. Grzesik, and D. Philipp, "Influence of mechanical load at low temperatures on cell defects and power degradation at full scale PV modules," *Proc. 28th Eur. Photovolt. Sol. Energy Conf. Exhib.*, 2013, pp. 2968–2971. [Online]. Available: <https://userarea.eupvsec.org/proceedings/28th-EU-PVSEC/4DO.2.2/>